# Enhancement of solid-state proton NMR via SPINOE with laser-polarized xenon

Xin Zhou*, Jun Luo, Xian-ping Sun, Xi-zhi Zeng,

Shang-wu Ding, Mai-li Liu, Ming-sheng Zhan

*State Key Laboratory of Magnetic Resonance and Atomic and Molecular Physics,*

*Wuhan Institute of Physics and Mathematics,*

*The Chinese Academy of Sciences, P. O. Box 71010,*

*Wuhan 430071, People's Republic of China*

## Abstract

We have first successfully transferred the $^{129}$Xe polarization of natural isotopic composition to the proton of solid-state $^{1}$HCl via Spin Polarization-Induced Nuclear Overhauser Effect (SPINOE), by mixing the hyperpolarized $^{129}$Xe gas and the $^{1}$HCl gas and then cooling them to their condensated state in a flow system. The solid-state enhanced factor of the NMR signal of 6 for $^{1}$H was observed, and the equation of solid-state polarization enhancement via cross relaxation has also been theoretically deduced. Using this equation, the theoretically calculated enhancement is in agreement with the measured value within error. Also, this technique is maybe useful to establish a solid state NMR quantum computer.

PACS number(s): 32.80.Bx, 33.25.+k, 03.67.Lx

* Corresponding author. E-mail: xinzhou@wipm.ac.cn; Tel: +86-27-8719-7796; Fax: +86-27-8719-9291.

## I. INTRODUCTION

Many difficulties appear in scaling the liquid-state Nuclear Magnetic Resonance (NMR) quantum computers to multi-qubit, since the signal intensity is low sensitive and decreases exponentially with increasing the number of qubits. Therefore, the maximal number of qubits of quantum computer using the current liquid-state NMR technology might be limited to $10^1$. Although there are some methods developed for enhancing polarization, such as lower temperature and higher magnetic fields, Dynamic Nuclear Polarization (DNP)[2,3], Nuclear Overhauser Effect (NOE)[4], cross polarization[5], etc., unfortunately these approaches can provide only limited relief or need rigid conditions for polarization enhancement. A promising route to enhance the nuclear polarization is the utilization of optical pumping and spin exchange[6,7,8], which can increase the nuclear polarization by four or five orders of magnitude over thermal equilibrium. The hyperpolarized $^{129}$Xe and $^3$He gases are greatly effective in the development of magnetic resonance imaging[9], surface science[10], probing of biological system[11,12], polarized targets[13], neutron polarization[14], precision measurement[15], polymer science[16], quantum computation[17], etc..

Hitherto, proton sensitivity enhancements are not very large in all experiments[18,19,20,21] except for surface enhancements[22], and all of these experiments have almost been implemented by using gaseous or liquid hyperpolarized xenon. The $^1$H polarization has been enhanced by a factor of 0.1 to 2 on a 4.2T NMR spectrometer at room temperature via cross-relaxation between dissolved hyperpolarized gaseous $^{129}$Xe and $^1$H of the liquid benzene solvent, which has also been firstly called the SPINOE by Pines' group[19]. Through dissolving compounds in hyperpolarized liquid xenon, the enhanced signal of over 45 for $^1$H has also been observed at 1.4T and 200K by Happer's group[20]. In Xe ice, larger nuclear polarization of hyperpolarized $^{129}$Xe has been transferred to $^{13}CO_2$ by low-field thermal mixing[23]. However, as far as we know, solid-state proton polarization enhancement has not been reported in the literature.

Solid-state quantum computers, which could execute the $10^6$ qubits operation brought out by DiVincenzo *et al.*, were widely noticed[24]. Considering that hydrogen chloride (HCl) and xenon have almost the same melting points between 160 and 170K, and the longitudinal relaxation time ($T_1$) of hyperpolarized $^{129}$Xe in solid-state (4K) is about 500 hours[25], we put forward the idea of laser-enhanced solid-state quantum computer (LESSQC) by mixing

hyperpolarized $^{129}$Xe and $^{1}$HCl.

In this letter, we firstly demonstrate that the polarization of hyperpolarized solid-state $^{129}$Xe produced by spin exchange is transferred to the proton of solid-state $^{1}$HCl via SPINOE without using low-field thermal mixing or Hartmann-Hahn matching condition. This method yields the proton enhancement of 6 by comparison of that without optical pumping on a Bruker SY-80M NMR spectrometer (1.87T) at 142 K, leading us to take a step towards realizing LESSQC.

## II. EXPERIMENT AND RESULTS

The experimental apparatus, similar to that in Ref. 26, is shown schematically in Figure 1. Briefly, the whole system consists of an optical pumping system (the right part of the valve K4), which is used to produce the hyperpolarzied gaseous $^{129}$Xe, and a cross-relaxation and detection system (the left part of the valve K4). The two parts are connected by a cylindrical Pyrex tube and separated by stopcocks. The whole system was evacuated with K2, K5 valves closed and K1, K3 and K4 valves opened. When the vacuum reached to $1.5\times10^{-5}$ Torr for several hours, the valves K1, K4 and K5 were closed and K2 and K3 opened. The cylindrical pump cell containing a few drops of metal Cs, with a volume of 600 cm$^3$, was loaded 760 Torr natural isotopic xenon gas at room temperature and an atmosphere, then all valves were closed. The pump cell, which was placed in a 25 Guass magnetic field generated by Helmholtz coils, was maintained at approximately 333$\pm$4 K by a resistance heater (not shown) during the optical pumping. The inner surfaces of the cylindrical Pyrex tube and the pump cell were coated with silane in order to slow down the relaxation of the $^{129}$Xe upon collision with the tube wall. As soon as all valves were closed, laser light from a 15 W cw tunable semiconductor-diode laser array (Opto Power Co. Model OPC-D015-850-FCPS) at wavelength $\lambda$=852.1 nm was introduced to the system. After passing through beam expander, Glan prism, $\lambda/4$ plate and convex lens, the laser light became circularly polarized, and illuminated almost 4/5 of the pump cell volume. The propagation of the laser paralleled to the orientation of the magnetic field B. The circularly polarized laser resonates with the Cs $D_2$ absorption line and induces an electron spin polarization in the Cs atoms via a standard optical pumping process[7,8]. After about 25 minutes, the hyperpolarized $^{129}$Xe gas was produced by spin-exchange collision with the Cs atoms.

At the part of cross-relaxation and detection system, there were a liter of $^{1}$HCl gas at room temperature and an atmosphere in the tank. K4 and K5 valves were opened to allow the hyperpolarized $^{129}$Xe and $^{1}$HCl to be mixed, then transferred to the NMR sample probe (10 mm diameter, 8 mm inner diameter), pre-cooled to 172±2 K, of the Bruker SY-80M NMR spectrometer. The temperature of the probe was subsequently reduced to 142 K in an evacuated glass dewar by flowing cold nitrogen gas from liquid nitrogen tank, which controlled by the Bruker variable temperature unit. This temperature was kept, and the variation was less than 2 K at all times so that the mixture could be in the solid-state. Since there exist imbalance of polarization, the hyperpolarized $^{129}$Xe and the thermally polarized proton, in the mixed system, the interaction between the $^{129}$Xe and the proton can make spin exchange occur via SPINOE.

The time dependence of the $^{129}$Xe NMR signal intensity (solid circle) observed after blending hyperpolarized $^{129}$Xe and $^{1}$HCl is shown in Figure 2(a). The observed spin-lattice relaxation time of $^{129}$Xe in the presence of $^{1}$HCl is 29.6±0.6 min. The initial rise of signal manifests the accumulation of solid-state hyperpolarized $^{129}$Xe in the probe, similar to that in Ref. 19. At the peak signal, the increase of accumulated $^{129}$Xe magnetization reaches a balance with the decay of $^{129}$Xe magnetization via SPINOE with $^{1}$HCl. After this peak point, $^{129}$Xe magnetization decays as a result of SPINOE. So the solid line, a fit to data after the peak, represents the time dependence of $^{129}$Xe residual magnetization after a SPINOE experiment.

Figure 2(b) displays the time dependence of the solid-state proton NMR signal (solid circle) from the same run. Both the accumulation of the condensed state mixture and the cross-relaxation between the proton and the hyperpolarized $^{129}$Xe contribute to the initial rise of the proton signal. The proton NMR signal reaches its peak vaule at a time t=280 s after the mixing, and decays towards its thermal equilibrium value (dashed line) at the same rate as $^{129}$Xe signal. The solid line represents a fit to data to guide eyes. We used pulse flip angles of $4^0$ and $9^0$ for $^{129}$Xe and $^{1}$H respectively, and $^{129}$Xe was performed with a home-bulit probe.

Typcial spectrum for the enhanced proton is shown in Figure 3. In order to obtain the large $^{1}$H NMR signal, we used $90^0$ pulse angle for a single acquisition at a time t=280 s. Figure 3(b) presents a typical enhanced $^{1}$H NMR spectrum comparing with the one at thermal equilibrium (Figure 3(a)). Due to the relation of the magnetization versus the

nuclear spin polarization given by Abragam[2], the enhancement factor of the solid-state $^1$H was about 6, which corresponds to the proton polarization of $8.55\times10^{-5}$, on the basis of compariosn of the integrated intensity of the laser-enhanced signal with that at equilibrium.

## III. THEORETICAL ANALYSIS AND DISCUSSION

The interactions are complicated in solid-state, but in this paper, we will limit our discussion to only spins-$\frac{1}{2}$ nuclei coupled via the direct nuclear dipolar interaction:

$$H_D = \frac{\gamma_S \gamma_I}{r^3}[S \bullet I - 3(r \bullet S)(r \bullet I)], \tag{1}$$

where $I$ and $S$ are the spin angular momentum operators, $\gamma_I$ and $\gamma_S$ are the gyromagnetic ratios of I and S spins, respectively, and $r$ is the distance between two spins. Due to the perturbation of Hamiltonian $H_D$, the transition probabilities $W$ between the eigenstates can be given[27]:

$$\begin{aligned} W_0^{IS} &= \tfrac{2\delta}{20} J(\omega_I - \omega_S), \\ W_{1I}^{IS} &= \tfrac{3\delta}{20} J(\omega_I), \\ W_{1S}^{IS} &= \tfrac{3\delta}{20} J(\omega_S), \\ W_2^{IS} &= \tfrac{12\delta}{20} J(\omega_I + \omega_S), \end{aligned} \tag{2}$$

with

$$\delta = \frac{\hbar^2 \gamma_S^2 \gamma_I^2}{r^6}, \tag{3}$$

$$J(\omega) = \frac{\tau_c}{1 + \omega^2 \tau_c^2}, \tag{4}$$

here, $\hbar$ is the Planck constant divided by $2\pi$, and $\tau_c$ is the correlation time of spin systems.

Accroding to the Solomon equations, the evolution of this two-spin systems, $^1$H (I=$\frac{1}{2}$) and $^{129}$Xe (S=$\frac{1}{2}$), could be described by[2,27]:

$$\frac{d}{dt}\begin{pmatrix} I_z \\ S_z \end{pmatrix} = -\begin{bmatrix} \rho_I & \sigma_{IS} \\ \sigma_{SI} & \rho_S \end{bmatrix}\begin{pmatrix} I_z - I_0 \\ S_z - S_0 \end{pmatrix}, \tag{5}$$

where $I_z$ and $S_z$ are z components of the spins I and S respectively, $I_0$ and $S_0$ are their equilibrium values, $\rho_I$ and $\rho_S$ are the autorelaxation rates of the $^1$H and the $^{129}$Xe spins, and $\sigma_{IS}$ and $\sigma_{SI}$ are the corresponding cross-relaxation rates. The elements of cross-relaxation

matrix can be expressed by the transition probabilities W resulting from II, SS and IS interactions[28]:

$$\begin{aligned}\rho_I &= 2(n_I-1)(W_1^{II}+W_2^{II})+n_S(W_0^{IS}+2W_{1I}^{IS}+W_2^{IS}),\\ \rho_S &= 2(n_S-1)(W_1^{SS}+W_2^{SS})+n_I(W_0^{IS}+2W_{1S}^{IS}+W_2^{IS}),\\ \sigma_{IS} &= n_S(W_2^{IS}-W_0^{IS}),\\ \sigma_{SI} &= n_I(W_2^{IS}-W_0^{IS}),\end{aligned} \tag{6}$$

here, $n_I$ and $n_s$ are magnetically equivalent I and S spins. A solution of equation (5) of particular interest in this system is the one corresponding to the initial conditions:

$$\begin{aligned}(I_z-I_0)_{t=0} &= 0,\\ (S_z-S_0)_{t=0} &= S_i.\end{aligned} \tag{7}$$

So the solution can be given by:

$$\begin{aligned}I_z(t) &= I_0+C(\exp(\lambda_1\cdot t)-\exp(\lambda_2\cdot t)),\\ S_z(t) &= S_0+C[r_1\cdot(\exp(\lambda_1\cdot t)-r_2\cdot\exp(\lambda_2\cdot t))],\end{aligned} \tag{8}$$

where $\lambda_1$ and $\lambda_2$ are given by:

$$\begin{aligned}\lambda_1 &= \tfrac{-(\rho_I+\rho_S)-\sqrt{(\rho_I-\rho_S)^2+4\sigma_{IS}\sigma_{SI}}}{2},\\ \lambda_2 &= \tfrac{-(\rho_I+\rho_S)+\sqrt{(\rho_I-\rho_S)^2+4\sigma_{IS}\sigma_{SI}}}{2},\end{aligned} \tag{9}$$

and

$$\begin{aligned}r_1 &= \tfrac{\rho_S-\sqrt{(\rho_I-\rho_S)^2+4\sigma_{IS}\sigma_{SI}}}{2\sigma_{IS}},\\ r_2 &= \tfrac{\rho_S+\sqrt{(\rho_I-\rho_S)^2+4\sigma_{IS}\sigma_{SI}}}{2\sigma_{IS}},\end{aligned} \tag{10}$$

$$C = \frac{S_i}{r_1-r_2}. \tag{11}$$

Therefore, the $^1$H enhancemet via cross-relaxation comparing with that at thermal equilibrium is:

$$\frac{I_z(t)-I_0}{I_0} = -\frac{\sigma_{IS}}{\rho_I}\frac{\gamma_S}{\gamma_I}\frac{S_z(t)-S_0}{S_0}, \tag{12}$$

where $[S_z(t)-S_0]/S_0$, the enhancement of hyperpolarized solid-state $^{129}$Xe, is about 6000 in our experiment, which corresponds to the $^{129}$Xe polarization of 2.16%[26]. Inserting the values (2) and (6) into (12) we get:

$$\frac{I_z(t)-I_0}{I_0} = \frac{-\gamma_S(S_z(t)-S_0)n_S[6\delta J(\omega_I+\omega_S)-\delta J(\omega_I-\omega_S)]}{\gamma_I S_0\{(n_I-1)[3\delta' J(\omega_I)+12\delta' J(2\omega_I)]+n_S[\delta J(\omega_I-\omega_S)+3\delta J(\omega_I)+6\delta J(\omega_I+\omega_S)]\}}, \tag{13}$$

with

$$\delta' = \frac{\hbar^2 \gamma_I^4}{r'^6}, \tag{14}$$

here $r'$ is the distance between two neighboring I spins.

In our experiment, $\omega_I$ ($^1$H) and $\omega_S$ ($^{129}$Xe) are 80.13MHz and 22.16MHz (on Bruker AC-80 spectrometer). The concentrations of $^1$H and $^{129}$Xe are 34.6mmol/cm$^3$ and 5.46mmol/cm$^3$ respectively. We can image a model that one $^{129}$Xe nucleus is surrounded by six $^1$H nuclei on average. The autorelaxation rate of the proton $\rho_I$ of $(66\ \mathrm{s})^{-1}$ is measured in the experiment so that one can obtain the cross relaxation $\sigma_{IS}$ by the equation (12). Therefore, the correlation time $\tau_c$ is estimated to be $6.18\times10^{-5}$ s. Using the equation (6), we can calculate that autorelaxation rates $\rho_I$ and $\rho_S$ are $(81\ \mathrm{s})^{-1}$ and $(62\ \mathrm{min})^{-1}$, and cross relaxation rates $\sigma_{IS}$ and $\sigma_{SI}$ are $5.53\times10^{-5}$ s$^{-1}$ and $3.32\times10^{-4}$ s$^{-1}$, respectively. Thus from equation (8), the time evolution of the proton polarization can be theoretically writen as:

$$I_z(t) = I_0 + C(\exp(-t/3744) - \exp(-t/81)). \tag{15}$$

The theoretical simulation (dot line) is visualized in Figure 2(b) for clear comparison to experimental results. Although only the direct nuclear dipolar interaction is considered in the above discussion, in fact, there are so many factors, such as spin rotation, paramagnetisim, relaxation with the wall, inhomogenuous magnetic field, etc., which can induce the relaxation. Consequently the theoretical relaxation rates are smaller than the experimental ones, and predictions of the time dependence of the proton polariztion are larger than experimental results.

Assuming $r$ is equal to $r'$ for simplification in our theoretical model, one can calculate the maximum solid-state proton enhancement of 7.1 using equation (13), which is in general agreement with the measured value. Although it is substantially smaller than the $^{129}$Xe enhancement, this can not indicate the possibility that only a fraction of the total number of $^1$HCl molecules interact with the hyperpolarized $^{129}$Xe by diploar-diploar. Because only the natural xenon (26.4% enriched $^{129}$Xe, 21.2% enriched $^{131}$Xe) has been used, at the temperature of 142K, the cross-relaxation between $^{129}$Xe and the isotope $^{131}$Xe can decrease the efficiency of polarization transfer from $^{129}$Xe to $^1$H[25]. On the other hand, dipolar relaxation from diffusing vacancies dominates at this temperature for $^{129}$Xe spin-lattice relaxation[29]. If we take into account of all above factors, together with the inhomogenuous magnetic field due to the fluctuation of eletromagnet and the polarization loss during the phase transition,

etc., all of these losses maybe counterbalance the difference between experimental values and theoretical ones.

According to equation (13), for further increasing the proton enhancement, one should first obtain the greatest $^{129}$Xe enhancement via employing the high power and narrow bandwidth laser, and/or increase the gas pressure of the pump cell in order to enhance the optical-pumped absorbed power when using the wide bandwidth laser. A small proton number density by using partially deuterated sample and a large $^{129}$Xe number density by using Xe isotopically enriched with $^{129}$Xe also can boost transfer efficiency.

## IV. CONCLUSION

In conclusion, we firstly obtained the solid-state laser-enhanced NMR proton signal of $^{1}$HCl via SPINOE by cooling hyperpolarzied $^{129}$Xe to solid-state at 1.87T and 142K in the flow system. The amplification factor of the proton nuclear polarization is about 6. The theoretical calculated enhancement is in agreement with the measured value. Furthermore, the hyperpolarized $^{129}$Xe has long lifetime in the solid-state, which means that $^{1}$H could keep the longer coherence time with hyperpolarized $^{129}$Xe. Therefore this method may be useful to overcome one of the difficult problems in liquid-state NMR quantum computer and to establish solid-state quantum computers.

Solid-state signal enhancement via SPINOE with hyperpolarized $^{129}$Xe is not limited to the proton, i.e., it can be expanded to other nuclei. Although we have focused on quantum computers, this method should be readily extended to material science and determination of the 3D structure of large biomolecules, since NOE can provide unique information on molcular structure which can not be obtained with any other known technique. Traditional NOE needs to irradiate one nucleus in order to observe anther. However, it is very convenient and available for probing interactions between nuclei without any additional conditions by using this method.

## V. ACKNOWLEDGMENT

This work is supported by the National Natural Science Foundation of China under Grant No. 10234070, National Science Fund for Distinguished Young Scholars un-

der Grant No. 29915515 and National Fundamental Research Program under Grant No. 2001CB309306.

---

[1] W.S. Warren, Science **277**, 1688 (1997).

[2] A. Abragam, *The Principles of Nuclear Magnetism* (Oxford University Press, London, 1961).

[3] R.D. Bates, Magn. Reson. Rev. **16**, 237 (1993).

[4] A. Overhauser, Phys. Rev. **89**, 689 (1953); **92**, 477 (1953).

[5] C. P. Slichter, *Principles of Magnetic Resonance*, Springer Series of Solid State Sciences, **Vol. 1** (Springer-Verlag, Berlin,1990).

[6] W. Happer, E. Miron, S. Schaefer, D. Schreiber, W. A. van Wijngaarden, and X. Zeng, Phys. Rev. A **29**, 3092 (1984).

[7] X. Zeng, Z. Wu, T. Call, E. Miron, D. Schreiber, and W. Happer, Phys. Rev. A **31**, 260 (1985).

[8] T. G. Walker, W. Happer, Rev. Mod. Phys. **69**, 629 (1997).

[9] M. S. Albert, G. D. Cates, B. Driehuys, W. Happer, B. Saam, C. S. Springer, A. Wishnia, Nature **370**, 199 (1994).

[10] T. Pietrass, A. Bifone, and A. Pines, Surf. Sci. **334**, L730 (1995).

[11] S. M. Rubin, M. M. Spence, A. Pines, and D. E. Wemmer, J. Magn. Reson. **152**, 79 (2001).

[12] A. Cherubini, A. Bifone, Prog. Nucl. Magn. Reson. Spectrosc. **42**, 1 (2003).

[13] W. Xu *et al.*, Phys. Rev. Lett. **85**, 2900 (2000).

[14] G. Jones, T. Gentile, A. Thompson, Z. Chowdhuri, M. Dewey, W. Snow, and F. Wietfeldt, Nucl. Instrum. Methods Phys. Res., Sect. A **440**, 772 (2000).

[15] D. Bear, R. E. Stoner, R. L. Walsworth, V. A. Kostelecky, and C. D. Lane, Phys. Rev. Lett. **85**, 5038 (2001).

[16] B. Nagasaka, H. Omi, T. Eguchi, H. Nakayama, and N. Nakamura, Chem. Phys. Lett. **340**, 473 (2001).

[17] A. S. Verhulst, O. Liivak, M. H. Sherwood, H. M. Vieth, and I. L. Chuang, Appl. Phys. Lett. **79**, 2480 (2001).

[18] Y. Q. Song, Concepts Magn. Reson. **12**, 6 (2000).

[19] G. Navon, Y. -Q. Song, T. Room, S. Appelt, R. E. Taylor, A. Pines, Science **271**, 1848 (1996).

[20] R. J. Fitzgerald, K. L. Sauer, W. Happer, Chem. Phys. Lett. **284**, 87 (1998).

[21] T. Rõõm, S. Appelt, R. Seydoux, E.L. Hahn, A. Pines, Phys. Rev. B **55**, 11604 (1997).

[22] B. Driehuys, G.D. Cates, W. Happer, H. Mabuchi, B. Sasm, M.S. Albert and A. wishnia, Phys. Lett. A **184**, 88 (1993).

[23] C. R. Bowers, H. W. Long, T. Pietrass, H. C. Gaede and A. Pines, Chem. Phys. Lett. **205**, 168 (1993).

[24] D. P. DiVincenzo, Science **270**, 255 (1995).

[25] M. Gatzke, G.D Cates, B. Driehuys, D. Fox, W. Happer, B. Saam, Phys. Rev. Lett. **70**, 690 (1993).

[26] X. Zhou, J. Luo, X. Sun, X. Zeng, M. Liu and W. Liu, Acta Physica Sinica (*in Chinese*) **51**, 2221 (2002).

[27] I. Solomon, Phys. Rev. **99**, 559 (1955).

[28] R. R. Ernst, G. Bodenhausen, and A. Wokaun, *The Principles of Nuclear Magnetic Resonance in One and Two Dimensions* (Oxford University Press, London, 1987).

[29] G. D. Cates, D. R. Benton, M. Gatzke, W. Happer, K. C. Hasson, and N. R. Newbury, Phys. Rev. Lett. **65**, 2591 (1991).

# Figure captions

Fig. 1. Schematic diagram of the experimental setup.

Fig. 2. (a) Time dependence of the solid-state $^{129}$Xe NMR signal (solid circle) observed after the blend of hyperpolarized $^{129}$Xe and $^{1}$HCl at 142 K and 1.87 T. The solid line, a fit to data after the peak, represents how much $^{129}$Xe magnetization is left after a SPINOE experiment. (b) Time dependence of the solid-state proton NMR signal (solid circle) from the same sample, and it relaxes towards its thermal equilibrium value (dashed line). The dot line represents the theoretical predictions for comparison to experimental results (solid line).

Fig. 3. (a) The solid-state proton NMR spectra of $^{1}$HCl under the conditions of thermal equilibrium and (b) laser-enhanced signal via SPINOE with hyperpolarized $^{129}$Xe.

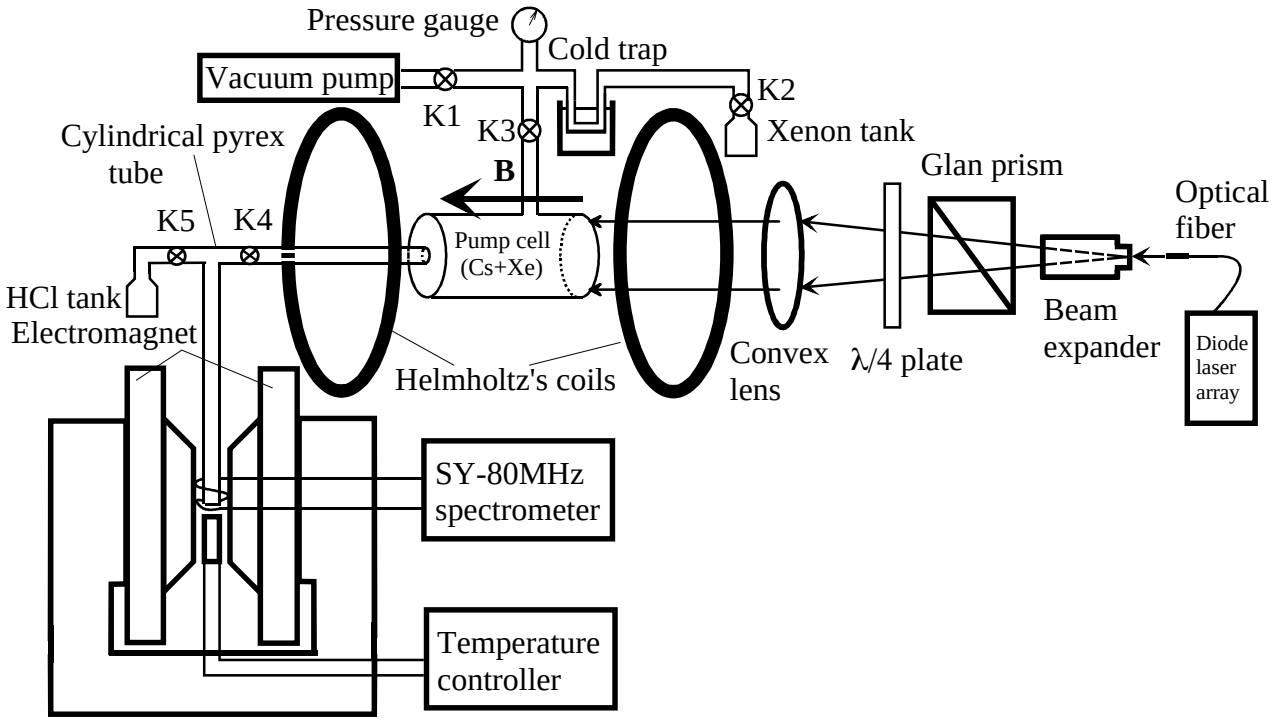
Pressure gauge
Cold trap
Vacuum pump
K1
K2
K3
Xenon tank
Cylindrical pyrex tube
B
Glan prism
Optical fiber
K5
K4
Pump cell (Cs+Xe)
HCl tank
Electromagnet
Helmholtz's coils
Convex lens
λ/4 plate
Beam expander
Diode laser array
SY-80MHz spectrometer
Temperature controller

**Figure 1**

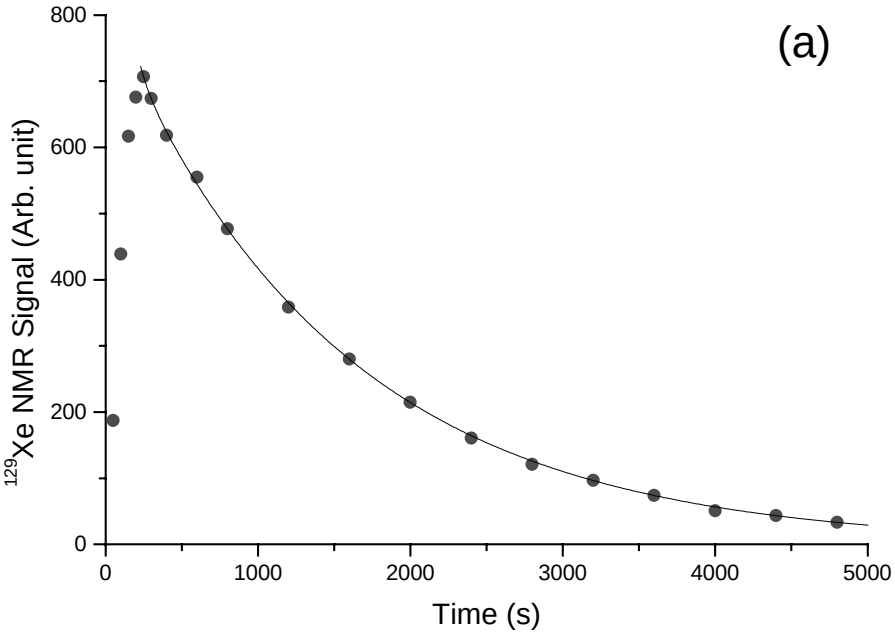
(a)
800
600
400
200
0
$^{129}$Xe NMR Signal (Arb. unit)
0
1000
2000
3000
4000
5000
Time (s)

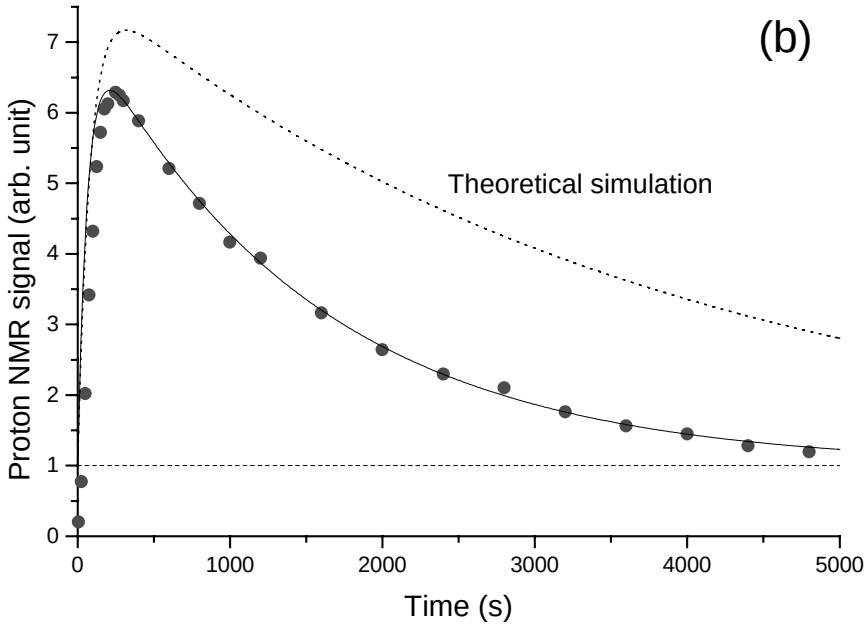
(b)
7
6
5
4
3
2
1
0
Proton NMR signal (arb. unit)
Theoretical simulation
0
1000
2000
3000
4000
5000
Time (s)

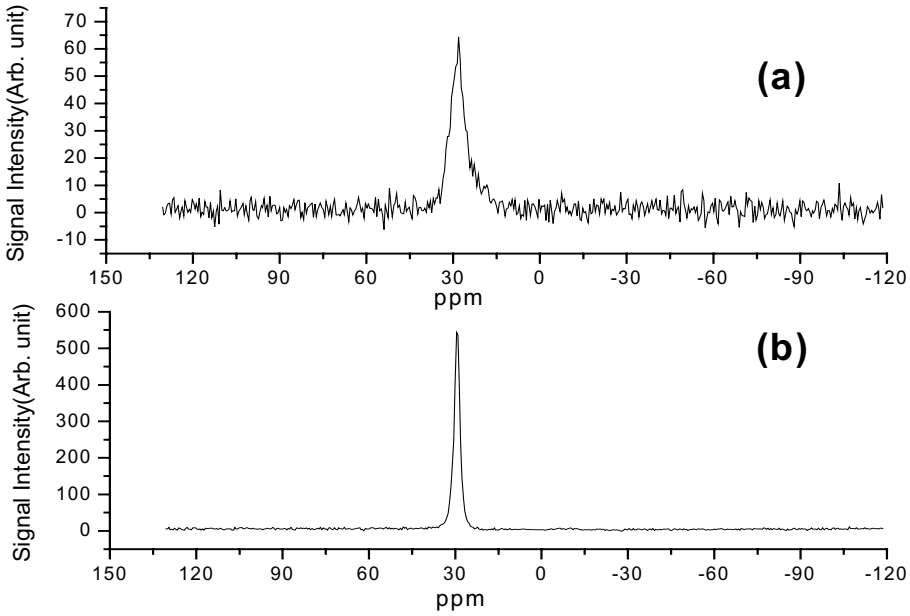
Signal Intensity(Arb. unit)
70
60
50
40
30
20
10
0
-10
150
120
90
60
30
0
-30
-60
-90
-120
ppm
(a)
Signal Intensity(Arb. unit)
600
500
400
300
200
100
0
150
120
90
60
30
0
-30
-60
-90
-120
ppm
(b)

**Figure 3**